A Novel Finger Kinematic Tracking Method Based on Skin-Like Wearable Strain Sensors

Shanshan Yao, Luis Vargas, Xiaogang Hu, and Yong Zhu, *Member, IEEE*

Abstract—Deficits in hand function are common in a majority of stroke survivors. Although hand performance can be routinely assessed during rehabilitation training, a lack of hand usage information during daily activities could prevent clinicians or therapists from making informative therapeutic decisions. In this paper, we demonstrated and validated the application of silver nanowire-based capacitive strain sensors for finger kinematic tracking. The fabricated strain sensors show high sensitivity (gauge factor close to one), low hysteresis, good linearity, large stretchability (150%), and skin-like mechanical property (Young's modulus of 96 kPa). All these features allow the sensors to be conformally attached onto the skin to track finger joint movement with minimal interference to daily activities. Recordings of the skin deformation from the strain sensors and joint angles from reflective markers are highly correlated (>93%) for different joint oscillation speeds in a stroke survivor and a control subject, indicating the high accuracy of the strain sensors in joint motion tracking. With the wearable silver nanowire-based strain sensors, accurate hand utility information on the impaired hand of stroke survivors can be acquired in a continuous and unobtrusive manner.

Index Terms—Wearable sensors, strain sensors, finger kinematic tracking, stroke, hand function impairment.

I. INTRODUCTION

HEMISPHERIC strokes occur in approximately 15 million individuals worldwide each year [1]. Following a chronic stroke, muscular deficiency can emerge limiting mobility in stroke survivors. This condition is known as hemiparesis that can result in difficulty during the manipulation of one side of the individual's body. Information on the movement of individual joints is critical for rehabilitation. Many joints located along the arms and legs (i.e., shoulders and knees) can be evaluated using wearable

S. Yao is with the Department of Mechanical and Aerospace Engineering, North Carolina State University, Raleigh, NC 27695 USA (e-mail: syao2@ncsu.edu).

L. Vargas and X. Hu are with the Joint Department of Biomedical Engineering, University of North Carolina at Chapel Hill, Chapel Hill, NC 27599 USA, and also with North Carolina State University, Raleigh, NC 27695 USA (e-mail: lgvargas@ncsu.edu; xiaogang@unc.edu).

Y. Zhu is with the Department of Mechanical and Aerospace Engineering, North Carolina State University, Raleigh, NC 27695 USA, also with the Joint Department of Biomedical Engineering, University of North Carolina at Chapel Hill, Chapel Hill, NC 27599 USA, and also with North Carolina State University, Raleigh, NC 27695 USA (e-mail: yong_zhu@ncsu.edu).

devices that do not affect the motion of the limb [2]. Unfortunately, the evaluation of hand motion in a real-world environment is challenging because of the limited space, multiple joints, and degrees of freedom that are present. Rehabilitation of the hand requires the ability to track the quality of hand usage during daily activities, which allows clinicians to help address possible concerns or make necessary adjustments for rehabilitation purposes. The ability to track the hand performance using wearable devices is essential for providing accurate diagnostic results during daily use, which has yet been achieved. There are currently no existing wearable systems that are capable of tracking individual joints of the hand outside a clinical setting. Sensors, such as goniometers, accelerometers, or inertial sensors are often used for measuring changes in angle and position in other parts of the body, but when it comes to the hand these devices are bulky and typically affect the mobility of fingers and can cause a physical burden to the users [3], [4]. In the clinical setting, optical motion tracking systems are used to track various joints in the hand. These systems do not restrict any motion of the fingers or hand. However, the markers attached to the subject must remain in a given region based on the cameras' field of view. These limitations restrict the ability to create a wearable system that can continuously monitor the hand performance in real-world environments.

Truly wearable sensors that can deform in response to human motion and be conformal to curvilinear human skin promise a compelling future of personal health monitoring and activity tracking. Human skin is compliant with Young's moduli of epidermis and dermis in the ranges of 140 to 600 kPa and 2 to 80 kPa, respectively [5]. Skin itself can be elastically stretched up to 15%. Due to the existence of deformable structures (e.g. wrinkles and creases), skin can accommodate large strains involved in human motions up to 100%, especially for parts like knees and elbows [6]. Thus, in order not to affect daily activities, the sensors need to be highly compliant and stretchable. Nanomaterials have superior material properties, large surface areas, and are excellent candidates as building blocks for fabricating wearable sensors. Notably, highly compliant wearable sensors based on various nanomaterials such as silver nanowires (AgNWs), carbon nanotubes and graphene are rapidly emerging. Nanomaterial-enabled wearable strain sensors have shown great potential in health monitoring and activity tracking, such as monitoring pulse rate, respiration rate and body motions (e.g. finger bending, knee motions, and phonation vibrations) [7], [8]. In spite of the exciting progress, the accuracy of the strain sensors in monitoring

large body motions has yet been validated. Moreover, such wearable strain sensors have not been demonstrated for stroke survivors or other individuals with deficits in body movement.

This paper reports the application of a novel capacitive strain sensor based on AgNWs for hand kinematic tracking. The strain sensor is highly compliant and stretchable and can self-adhere to the skin, forming a conformable contact with skin. As a result, the strain sensor can reliably measure the skin deformation during joint movements without interfering with daily activities. The accuracy of the strain sensor based motion tracking method was rigorously validated by comparing it against the standard optical motion tracking method on both neurologically-intact and stroke subjects.

II. MATERIALS AND METHODS

A. Subject Recruitment

Two subjects were recruited for this study to provide initial validation of the AgNW strain sensors. One healthy control subject and one stroke survivor (7 years post stroke) were recruited to evaluate the use of the sensor and provide possible comparison in these two types of individuals. All participants were given informed consent via protocols approved by the Institutional Review Board at University of North Carolina – Chapel Hill.

B. Experimental Setup

Fabrication of the capacitive strain sensors follows our previous papers with modifications (Fig. 1) [9], [10]. Here a more compliant material (Ecoflex 0030®, Smooth-On, Inc.) was used to embed AgNWs, which reduces the overall modulus and improves the sensing range of the capacitive strain sensors. The failure strains of Ecoflex® 0010 and 0030 are around 900% and 800%, respectively [11]. To fabricate the sensor, polyimide masks with rectangular grooves were first prepared by cutting Kapton tapes using CAMEO® (Silhouette America, Inc., Lindon, Utah). After attaching the patterned masks onto a substrate, AgNWs dispersed in ethanol were drop casted into the grooves. The solvent was evaporated by heating on a hot plate at 50 °C. After peeling off the polyimide mask, liquid Ecoflex® 0030 (Smooth-On, Inc.) (part A to part B ratio of 1 : 1 by weight) was casted on top of the patterned AgNW strips, followed by curing the liquid at RT for 4 h. Next, the AgNW/Ecoflex composites with AgNW embedded just below the surface of Ecoflex were cut into desired shapes and peeled off the substrate. To make conformal interconnets for measurements, Eutectic gallium-indium (EGaIn, Aldrich, ≥99.99%) was applied to the end of the AgNW/Ecoflex strips and wired with a thin copper wire. Two identical pieces of AgNW/Ecoflex conductors were then sandwiched by a thin layer of liquid Ecoflex® 0010 (Smooth-On, Inc.) to serve as a stretchable dielectric. The structure was cured at RT for 4 h. A thin layer of stretchable adhesive made by mixing slacker (Smooth-On, Inc.) and Ecoflex with a weight ratio of 1:1 was applied onto the fabricated strain sensors followed by curing at RT for 6 h. The resulting strain sensors are self-adhesive, compliant and highly stretchable.
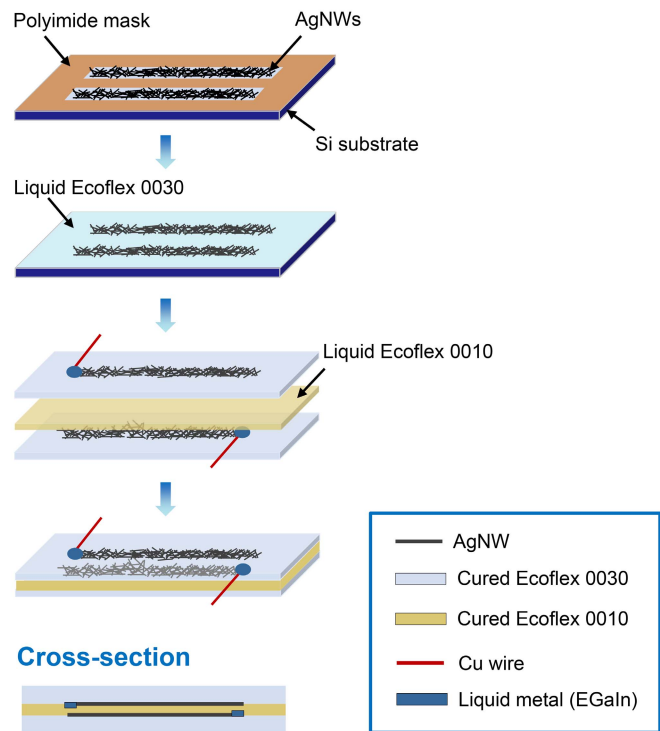

Fig. 1. Schematic illustration of the strain sensor fabrication process and the cross-sectional view of the sensor structure. Step 1: Drop cast AgNW/ethanol solution into the area defined by the polyimide shadow mask followed by evaporating the ethanol on a hot plate. Step 2: Drop cast liquid Ecoflex 0030 over the patterned AgNW conductors and cure the Ecoflex. Peel off the AgNW/Ecoflex 0030 film from the Si substrate. Step 3: Drop liquid metal (EGaIn) to make conformal contact with the terminals and connect thin copper lead wires to the AgNW conductors via the liquid metal. Sandwich two AgNW/Ecoflex 0030 films with a layer of liquid Ecoflex 0010 in between as the dielectric. Step 4: Cure the whole structure at room temperature to finish the fabrication. Note the legend refers only to the last two steps and the cross-sectional view. The schematics are not drawn to scale for illustration purpose.

Stress-strain curves for the fabricated AgNW capacitive strain sensors were tested using a mechanical tester (DTS Company, Menlo Park, CA). Since the strain involved with human motions is typically lower than 100%, [6] a maximum strain of 150% was applied to evaluate the mechanical properties of the strain sensors under different strain rates and during multiple stretching-releasing cycles. The loading speed varied from 0.1 mm s^{-1} to 2.5 mm s^{-1} to achieve strain rates from 0.01 s^{-1} to 0.25 s^{-1}. A 5 N load cell was used with a load cell sensitivity of 15.98 N/V. To access the sensitivity of the strain sensors, the capacitance was measured simultaneously during the stress-strain testing using a capacitance-to-digital converter (AD7152, Analog Devices, Norwood, MA) with a sampling frequency of 50 Hz. Relative capacitive change as a function of tensile strain was plotted as the calibration curve (see Fig. 4A as an example).

For finger joint motion tracking, individual strain sensors were placed to the dorsal side of the finger, crossing the joints of individual fingers (Fig. 2) to monitor the skin deformation. The joint angles associated with the movement of the hand were calculated from the data acquired from an 8-camera

Fig. 2. A strain sensor and reflective markers mounted on the hand of a stroke subject.

Optitrack System (Natural Point, Inc., Corvallis, OR). The camera system can be used to track the location of various IR reflective markers in a given field of view. The markers, 6 mm in diameter, were placed along each subject's hand on each joint of their fingers and thumb. Additional markers were placed on the metacarpals and distal phalanx of each digit. This motion capture system records the 3D position of each marker in real time at a 100 Hz sampling rate. The data obtained from the markers was initially processed using the Motive software. Afterwards, the motion capture data was taken from the Motive software and imported into MATLAB where the angle of each joint over time could be calculated. The position of the marker in the 3D space was used for determining the joint angle at each time point. The angle was calculated by applying inverse kinematics to the marker triplet associated with the joint of interest. The change in angle over time was compared to the change in %strain seen in the AgNW sensor to validate the correlation that was present between these two parameters. The correlation was used to evaluate the validity of the strain sensor for joint angle tracking.

C. Protocol

Participants were instructed to voluntarily produce oscillatory flexion-extension movements of the recorded joints covering the active range of motion of each joint. The flexion-extension angles of a total of 10 joints were measured, including the metacarpophalangeal (MCP) and proximal interphalangeal (PIP) joints of the four fingers, as well as the MCP and PIP joints of the thumb. The distal interphalangeal (DIP) joint was not measured, because this joint is typically correlated with the MCP or PIP joints [12], [13].

The participants were asked to produce oscillatory motions at three speeds: at their preferred speed, at a slower speed, and at a faster speed. For each oscillatory speed, one minute of recordings from the cameras was performed. The actual number of repetitions depended on the oscillation speed. The marker data were down-sampled to 50 Hz to match the

sampling rate of the capacitance data. For each 1-minute trial, a total of 3000 (50 Hz × 60 s) data points were used for the correlation between the skin strain measured from the strain sensors and the joint angles from the motion-capturing cameras.

A 1-minute rest was taken between trials to minimize fatigue, and additional resting time was also provided upon request. During the experiment, all the un-instructed joints were allowed to move, without physical constraints. The affected and contralateral hands of the stroke survivor were tested, and the dominant hand of the control subject was tested.

III. RESULTS

As shown in the stress-strain curves (Fig. 3), the strain sensor displays elastic behavior for strain up to 200% followed by a nonlinear region. The linear region allows the Young's modulus to be calculated via Hooke's law: $E = \sigma/\varepsilon$, where σ is the applied stress and ε is the resultant strain. The Young's modulus was found to be 91.5 kPa for this sensor and 96.3 ± 5.8 kPa (in average) for all the sensors used in this work. The stress-strain curves remained linear up to 150% strain under different strain rates ranging from 0.01 s^{-1} to 0.25 s^{-1}. Negligible change in the stress-strain curves was observed for different strain rates. Cyclic testing was performed to evaluate the stability of the strain sensors. The change in Young's modulus was within 5 kPa during 1000 cycles of loading and unloading.

The strain sensor is a stretchable parallel-plate capacitor [9], [14]–[19]. For a capacitor with initial length, width and separation between two electrodes of l_0, w_0 and d_0, respectively, and Poisson's ratio of v, under a tensile strain of ε, the length increases to $(1+\varepsilon)l_0$, while the width decreases to $(1-v\varepsilon)w_0$ and the separation decreases to $(1-v\varepsilon)d_0$. The capacitance under the tensile strain of ε can be given by

$$C = \varepsilon_0 \varepsilon_r \frac{(1+\varepsilon)l_0(1-v\varepsilon)w_0}{(1-v\varepsilon)d_0} = (1+\varepsilon)C_0 \qquad (1)$$

where ε_0 and ε_r represent the dielectric constant for the vacuum and the dielectric layer, respectively; C_0 indicates the initial capacitance. The theoretical gauge factor (*GF*) for the capacitive strain sensor, defined by relative change in capacitance divided by the change in tensile strain, is thus calculated to be:

$$GF = \frac{(C-C_0)/C_0}{\varepsilon} = 1 \qquad (2)$$

Fig. 4A gives the calibration result for one capacitive strain sensor during strain loading and unloading. As expected, the capacitance increases following a linear relationship. *GF* of this strain sensor was 0.99 over a wide strain range up to 150%, very close to the theoretical value of 1. Variations in *GF* was within 0.03 during 1000 cycles of stretching and releasing (Fig. 4B). For all strain sensors fabricated, the average *GF* was 0.96 ± 0.03.

The strain sensor was mounted onto the finger joint when the finger was relaxed. Bending the finger joint led to decreased joint angle and increased strain across the finger joint. Fig. 4 shows the comparison between the skin deformation (i.e., strain) recorded from the AgNW strain sensors and
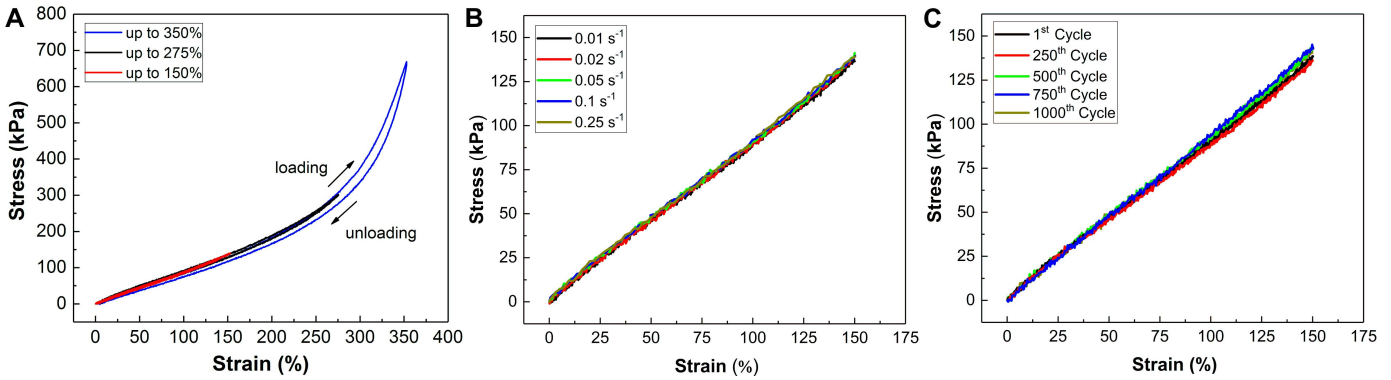
Fig. 3. (A) Stress-strain curves for the AgNW based strain sensor under different strain range at a strain rate of 0.01 s^{-1}. (B) Stress-strain curves for the AgNW based strain sensor under different strain rates. (C) Stress-strain curves for the AgNW based strain sensor during multiple cycles of stretching and releasing. The strain rate for cyclic testing was 0.25 s^{-1}.
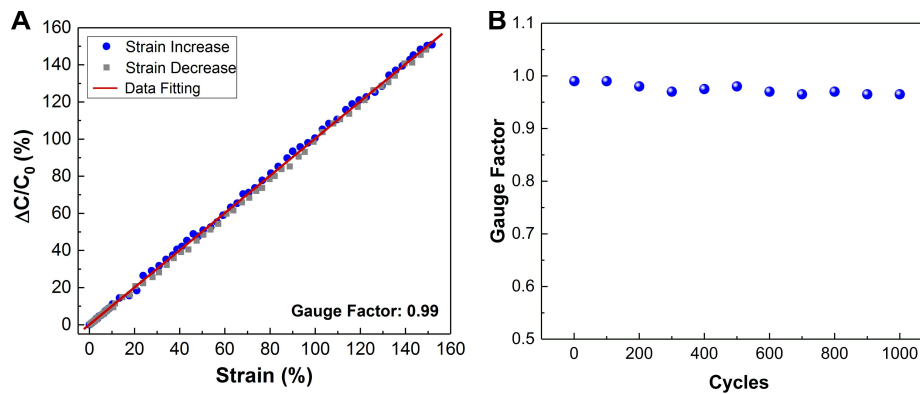

Fig. 4. (A) Relative capacitance changes as a function of applied tensile strain during strain loading and unloading. (B) Change in *GF* during multiple cycles of stretching and releasing.

the measured joint angles from the reflective markers using motion tracking cameras for both the stroke subject and the control subject. Pearson's correlation coefficient (r) between the signals from the two recordings (from capacitive sensors and cameras) was quantified for individual joint angles and at different joint oscillation speeds. The correlation coefficient r can be calculated using the following formula:

$$r = \frac{\sum_{i=1}^{n}(x_i - \bar{x})(y_i - \bar{y})}{\sqrt{\sum_{i=1}^{n}(x_i - \bar{x})^2}\sqrt{\sum_{i=1}^{n}(y_i - \bar{y})^2}} \quad (3)$$

where n is the sample size; x_i and y_i indicate the strain and angle, respectively; i represents individual sample; $\bar{x}$ and $\bar{y}$ are the sample mean values of strain and angle, respectively.

A ± 500 ms lag window was used to shift one recording source during the correlation in order to take into account potential sampling delays between the strain sensor recordings and the reflective marker data. The maximum correlation coefficient among the different lags was calculated as the correlation between the two recordings. The maximum correlation coefficient from an unimpaired control subject (Fig. 5A) is 0.98, and the maximum correlation coefficient from a stroke subject (Fig. 5B) is 0.93. As shown in Fig. 5C and 5D, the relationship between angle (θ) and strain (ε) can be expressed by $\theta = 170 - 1.30\varepsilon$ and $\theta = 168 - 1.39\varepsilon$ for the control subject and the stroke subject, respectively. Here the

unit of strain is in percentage. The correlations averaged across 10 finger joints for both subjects are 0.95 ± 0.03, 0.97 ± 0.03, and 0.96 ± 0.04, at slow, moderate, and fast speed oscillations, respectively. The overall correlation considering all the speeds is 0.96 ± 0.04 when averaged across the 10 finger joints.

IV. DISCUSSION

As shown in our case study, the AgNW based capacitive strain sensors indicate good linearity and negligible hysteresis. In contrast, resistive strain sensors often suffer from nonlinearity and large hysteresis [8], [20], which poses a challenge to real applications. The sensing range for the strain sensors (150%) are sufficiently larger than the strain level associated with human motions (typically < 100%). Table I summaries the performances of representative wearable capacitive strain sensors reported in literature. Our strain sensors showed improved sensitivity and sensing range than other capacitive strain sensors based on AgNW electrodes [9], [16], [21] and are among the best stretchable capacitive strain sensors reported to date [17], [19]. In addition to electrical performances, we demonstrated that the Young's moduli of our strain sensors are smaller than that of the epidermis, which indicates that our strain sensors are mechanically unperceivable to skins. With a skin-like modulus and larger strain range than that involved in human motions, the skin-attached strain sensors
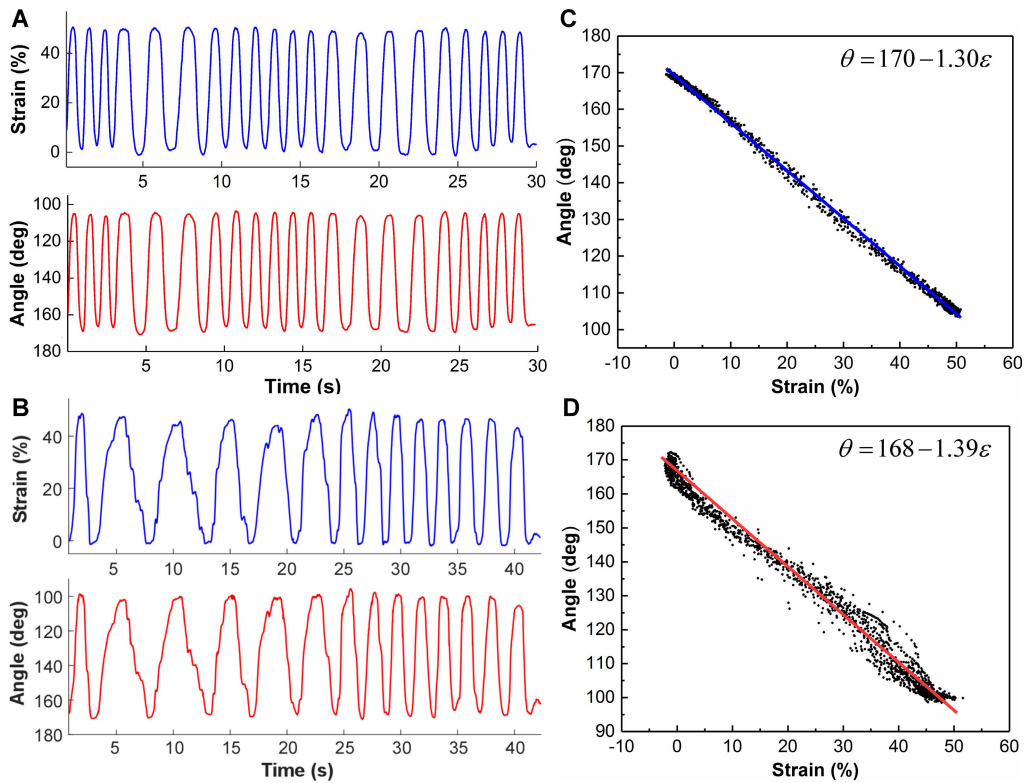
Fig. 5. (A): Skin strain involved in flexion-extension movements of the little finger recorded using an AgNW strain sensor (Top) compared with the estimated DIP joint angle from the reflective markers (Bottom) of a healthy control subject. (B): The comparison of a stroke survivor. (C) Angle versus strain curve for the control subject. (D) Angle versus strain curve for the stroke subject. The solid lines in (C) and (D) indicate the linear fitting results.

TABLE I

PERFORMANCES OF REPRESENTATIVE STRETCHABLE CAPACITIVE STRAIN SENSORS REPORTED

Structure	Young's Modulus	GF	Sensing Range	Linearity
AgNW-PDMS/Ecoflex/AgNW-PDMS [9]	-	0.7	50%	Linear
AgNW-PDMS/Ecoflex/AgNW-PDMS [16]	-	1	50%	Linear
AgNW-PU/Ecoflex/AgNW-PU [21]	-	0.5	60%	Linear
CNT-PDMS/Ecoflex/CNT-PDMS [14]	-	0.4	50%	Linear
CNT-silicone/silicone/CNT-silicone [18]	-	0.99	100%	Linear
CNT-PDMS/Dragon Skin/CNT-PDMS [19]	-	1	300%	Linear (after signal processing)
CNT-Ecoflex/Ecoflex/CNT-Ecoflex [17]	-	Around 1	150%	Linear
AgNW-Ecoflex/Ecoflex/AgNW-Ecoflex (this work)	**96.3 ± 5.8 kPa**	**0.96 ± 0.03**	**150%**	**Linear**

are mechanically invisible to the users, which is particularly important for continuous monitoring of stroke survivors who have reduced muscle strength. The sensors also keep the palmer side of the hand completely unobstructed, to avoid interfering with grasp actions and haptic sensing.

The correlation between the skin strain measured from the strain sensors and the joint angles from the motion cameras are higher than 93% at different joint oscillation speeds, for both subjects. The high correlation indicates the accuracy of the strain sensors in tracking finger joint motions across different movement conditions. In addition, the strain sensors showed sufficient resolution to capture the relatively slow and jerky motion of the finger joints of the stroke subject. Overall, the wearable tracking method can potentially provide

an efficient way for clinicians and therapists to evaluate the efficacy of the rehabilitation therapies, and to make timely and targeted adjustment of therapeutic strategies.

This new AgNW sensor has many potential applications for tracking joint kinematics in clinical populations by evaluating the user's quality of hand motion. This sensor addresses many of the limitations that are seen in other sensors. It can be applied along an individual's joint without restricting the movement of each finger and provides a low cost and accurate solution for use in obtaining data outside the clinical settings. One limitation of this study is the limited sample size. Future work will involve the use of a larger number of subjects to ensure that the measurements remain accurate and consistent with varying hand size, shape, and motion.

V. CONCLUSION

In conclusion, a novel finger movement tracking method based on wearable AgNW capacitive strain sensors was developed and validated. The sensors exhibited high sensitivity, low modulus, linear response, negligible hysteresis and large strain sensing range exceeding that involved in human motions. Due to the skin-like compliance and large stretchability, the strain sensors impose minimal constraint to the hand motion. High correlation between the recordings from the skin-mountable strain sensors and the standard optical motion tracking approach confirmed the accuracy of the strain sensors for finger movement tracking, based on the results from both neurologically-intact and stroke subjects. The results indicate that the AgNW strain sensor based tracking system is able to track the hand joint kinematics accurately. This wearable tracking system will also allow us to monitor hand performance in individuals with other chronic conditions such as cerebral palsy, spinal cord injury, or muscular dystrophy. The sensors can also be integrated into existing rehabilitation systems to track performance during hand therapy or be used as the input signals for virtual reality game based training. A plethora of wearable strain sensors have been developed over the past five years or so [8], [20], the work reported here can be used to evaluate and validate such strain sensors.

REFERENCES

[1] *The World Health Report 2002—Reducing Risks, Promoting Healthy Life*, World Health Organization, Geneva, Switzerland, 2002.

[2] H. Zheng, N. D. Black, and N. D. Harris, "Position-sensing technologies for movement analysis in stroke rehabilitation," *Med. Biol. Eng. Comput.*, vol. 43, no. 4, pp. 413–420, 2005.

[3] L. Wang, T. Meydan, and P. I. Williams, "A two-axis goniometric sensor for tracking finger motion," *Sensors*, vol. 17, no. 4, p. 770, 2017.

[4] H.-T. T. Chang, L.-W. A. Cheng, and J.-Y. J. Chang, "Development of IMU-based angle measurement system for finger rehabilitation," in *Proc. M2VIP*, Nanjing, China, Nov. 2016, pp. 1–6.

[5] D.-H. Kim *et al.*, "Epidermal electronics," *Science*, vol. 333, no. 6044, pp. 838–843, 2011.

[6] R. C. Webb *et al.*, "Ultrathin conformal devices for precise and continuous thermal characterization of human skin," *Nature Mater.*, vol. 12, pp. 938–944, Oct. 2013.

[7] T. Q. Trung and N.-E. Lee, "Flexible and stretchable physical sensor integrated platforms for wearable human-activity monitoringand personal healthcare," *Adv. Mater.*, vol. 28, no. 22, pp. 4338–4372, 2016.

[8] M. Amjadi, K.-U. Kyung, I. Park, and M. Sitti, "Stretchable, skin-mountable, and wearable strain sensors and their potential applications: A review," *Adv. Funct. Mater.*, vol. 26, no. 11, pp. 1678–1698, 2016.

[9] S. Yao and Y. Zhu, "Wearable multifunctional sensors using printed stretchable conductors made of silver nanowires," *Nanoscale*, vol. 6, no. 4, pp. 2345–2352, 2014.

[10] S. Yao *et al.*, "A wearable hydration sensor with conformal nanowire electrodes," *Adv. Healthcare Mater.*, vol. 6, no. 6, p. 1601159, 2017.

[11] *Ecoflex Series, Super-Soft, Addition Cure Silicone Rubbers*. Macungie, PA, USA: Smooth-On, Inc., 2017.

[12] E. J. Weiss and M. Flanders, "Muscular and postural synergies of the human hand," *J. Neurophysiol.*, vol. 92, no. 1, pp. 523–535, Jul. 2004.

[13] M. Santello, G. Baud-Bovy, and H. Jörntell, "Neural bases of hand synergies," *Frontiers Comput. Neurosci.*, vol. 7, p. 23, Apr. 2013.

[14] D. J. Lipomi *et al.*, "Skin-like pressure and strain sensors based on transparent elastic films of carbon nanotubes," *Nature Nanotechnol.*, vol. 6, pp. 788–792, Oct. 2011.

[15] S. Yao and Y. Zhu, "Nanomaterial-enabled stretchable conductors: Strategies, materials and devices," *Adv. Mater.*, vol. 27, no. 9, pp. 1480–1511, 2015.

[16] F. Xu and Y. Zhu, "Highly conductive and stretchable silver nanowire conductors," *Adv. Mater.*, vol. 24, no. 37, pp. 5117–5122, 2012.

[17] U.-H. Shin, D.-W. Jeong, S.-M. Park, S.-H. Kim, H. W. Lee, and J.-M. Kim, "Highly stretchable conductors and piezocapacitive strain gauges based on simple contact-transfer patterning of carbon nanotube forests," *Carbon*, vol. 80, pp. 396–404, Dec. 2014.

[18] D. J. Cohen, D. Mitra, K. Peterson, and M. M. Maharbiz, "A highly elastic, capacitive strain gauge based on percolating nanotube networks," *Nano Lett.*, vol. 12, no. 4, pp. 1821–1825, 2012.

[19] L. Cai *et al.*, "Super-stretchable, transparent carbon nanotube-based capacitive strain sensors for human motion detection," *Sci. Rep.*, vol. 3, Oct. 2013, Art. no. 3048.

[20] S. Yao, P. Swetha, and Y. Zhu, "Nanomaterial-Enabled wearable sensors for healthcare," *Adv. Healthcare Mater.*, vol. 7, no. 1, p. 1700889, 2018.

[21] W. Hu, X. Niu, R. Zhao, and Q. Pei, "Elastomeric transparent capacitive sensors based on an interpenetrating composite of silver nanowires and polyurethane," *Appl. Phys. Lett.*, vol. 102, no. 8, p. 083303, 2013.
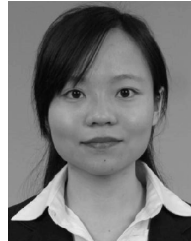
Shanshan Yao received the B.S. degree in microelectronics and the M.S. degree in microelectronics and solid-state electronics from Xi'an Jiaotong University in 2009 and 2012, respectively, and the Ph.D. degree in mechanical engineering from North Carolina State University in 2016. She is currently a Post-Doctoral Research Scholar with North Carolina State University. Her research interests include the growth, nanomechanics, and device applications of nanowires, and 2-D materials in flexible and wearable electronics.

Luis Vargas received the B.S. degree in mechanical engineering from the University of North Carolina at Charlotte in 2017. He is currently pursuing the Ph.D. degree in biomedical engineering with UNC/NC State, and is specializing in the research field of rehabilitation engineering. His research interests include neuro/biomechanics, stroke rehabilitation, and prosthetic/rehabilitation device design.

Xiaogang Hu received the B.E. degree in mechanical engineering from the Department of Precision Instruments and Mechanology, Tsinghua University, Beijing, China, in 2006, and the Ph.D. degree in kinesiology, with a focus on neural control of muscle force and a minor in computational science, from the Department of Aerospace Engineering, Pennsylvania State University, State College, PA, USA, in 2011. He was a Post-Doctoral Fellow at the Rehabilitation Institute of Chicago. He was a Research Scientist with the Rehabilitation Institute of Chicago and a Research Assistant Professor with the Department of Physical Medicine and Rehabilitation, Northwestern University. He is currently an Assistant Professor with the Joint Department of Biomedical Engineering, University of North Carolina at Chapel Hill and NC State University at Raleigh. His research interests are biosignal processing, stroke rehabilitation, and neuroprosthetics.

Yong Zhu (M'16) received the B.S. degree in mechanics and mechanical engineering from the University of Science and Technology of China in 1999, and the M.S. and Ph.D. degrees in mechanical engineering from Northwestern University in 2001 and 2005, respectively. He is currently a Professor with the Departments of Mechanical and Aerospace Engineering, Biomedical Engineering, and Materials Science and Engineering, North Carolina State University. His research interests include the mechanics of nanomaterials, micro/nano-electromechanical systems, and flexible/stretchable electronics.